Fundamental Study on Matching Stubs-Incorporated Probe-Fed Microstrip Patch Antenna

Takashi YANAGI, Yasuhiro NISHIOKA, Masataka OHTSUKA, and Shigeru MAKINO
Mitsubishi Electric Corporation
5-1-1 Ofuna, Kamakura, KANAGAWA, 247-8501 JAPAN, Yanagi.Takashi@bp.MitsubishiElectric.co.jp

Abstract

A novel antenna construction using the stubs formed on the patch conductor is proposed for broadening impedance bandwidth. The current distribution on the stubs and the patch conductor and the approximate circuit model for the proposed antenna structure is presented. Furthermore, the effectiveness of the proposed antenna construction and the influence on the radiation characteristic are investigated.

1. INTRODUCTION

The microstrip patch antennas (MSAs) are often used in various applications because of simple structure, low profile and low cost. In order to increase the bandwidth, many techniques have been proposed, which are classified roughly into three types. The first one is the methods of adding parasitic elements such as a co-planar [1] and a stacked [2] types. It is difficult to apply MSAs with coplanar parasitic elements to phased array antennas from a viewpoint of element-spacing. The second one makes slots [3] or slits [4] on the patch conductor. These methods do not allow us to use orthogonal polarizations simultaneously or wide-band circular polarization only by a single element. The last one utilizes a matching circuit as described in [5] which makes a large impact upon the area for RF and other circuits to be connected to the antenna element. Thus, the above methods restrict MSA's application fields, except for the MSA with stacked parasitic elements. The stacked MSA cannot always achieve broadbandness if the required thickness for the MSA is restricted, because there is an optimum distance between the driven and parasitic elements to obtain appropriate electromagnetic coupling between them.

On the other hand, L-shaped probe-fed MSA has been proposed [6], which can be classified into the third type. The parallel portion of the L-shaped probe to the patch conductor would form capacitive reactance with the length of less than $\lambda/4$. Since the vertical portion of the L-shaped probe has inductive reactance, the L-shaped probe would act a series resonant element. However, this structure usually needs the height of about $\lambda/10$ to obtain the probe's inductive reactance, where the height means the distance between the patch element and the ground plane. It is therefore considered that this technique cannot be applicable to thinner MSAs.

In this paper, we propose a new MSA construction method with a structure of impedance-matching function which is composed of two stubs mounted on the patch conductor. First, the surface current distribution on the stubs will be shown. Next, the approximate circuit model will be derived. Finally, the effectiveness of the proposed structure will be demonstrated numerically. The calculated results shown in this paper are obtained by a standard finite-difference time-domain (FDTD) method.

2. ANTENNA CONFIGURATION

Figure 1 shows the configuration of the proposed antenna structure. This antenna has two additional conductors except the patch conductor and the feeding probe. One is the conductor A, whose length is L_A ($<\lambda/4$) and width is W_A, is put above the patch conductor. The farthest edge of the conductor A from the probe is shorted to the patch conductor. The other is the conductor B, whose length is L_B ($<\lambda/4$) and width is W_B, is put above the conductor A. The conductor B is connected to the feeding probe. There is a small hole on the patch conductor to lead the feed-current to the conductor B along the probe. In this fundamental investigation, it is assumed that there are no dielectrics within and around the antenna and the size of the ground-plane is infinite.

3. ANALYSIS OF THE OPERATION

A. Current distribution

In order to understand the operation of the conductor A and B, the current distribution on the surfaces of the both conductors is analyzed by using the FDTD. The cell size is $\lambda/300$ and the computation space divided into $200 \times 200 \times 90$ cells is surrounded with the perfectly matched layer (PML). In this analysis, we concentrate our attention to the conductors-overlapped region for the purpose mentioned above. Figure 2 shows the x-component current distribution on each surface. The values of the magnitude and phase are represented by the colors and their correspondence is shown in the Figure. The amplitude of the current, including its distribution, on the upper surface of the patch conductor is nearly equal to that of the lower surface of the conductor A. On the other hand, their relative phase is different from each other approximately by 180^o. The almost same phenomenon can be seen for the overlapped region of the conductors A and B. The above analysis result indicates that each part of the conductors-overlapped region would act as a transmission line.

B. Approximate circuit model

If the conductor-overlapped region acts as a transmission line, the structure must be able to be replaced by a lumped circuit. In this section, we attempt to replace the stub structures by lumped element, and then derive an approximate circuit model.

Let us consider on the portion composed of the patch conductor and the conductor A. The impedance looking into the shorted conductor at the nearest edge from the feeding probe is given by

$$Z_A = jZ_{0A}\tan\left(\frac{2\pi}{\lambda}L_A\right) \quad (1)$$

where Z_{0A} is the characteristic impedance of the transmission line composed of the patch conductor and the conductor A. The equivalent inductance, L, for the transmission line at the edge can be estimated by

$$L = \frac{Z_A}{j\omega}. \quad (2)$$

Figure 3 shows the relationship between the antenna impedance at the natural resonant frequency of TM_{11} mode and the length of conductor A, L_A. The "conductor A model" means the results for the proposed structure without the conductor B, and the "equivalent L model" means the results when the conductor A is removed and the equivalent inductor is inserted between the patch conductor and the feeding probe. The height, H, denotes the distance between the patch conductor and the ground plane. The reactance values for the both models are in good agreement. Therefore, this part approximately operates as a so-called short-stub.

By a similar way, the conductor B is replaced with a lumped circuit. The impedance looking into the conductor B at the probe is given by

$$Z_B = \frac{Z_{0B}}{j\tan\left(\frac{2\pi}{\lambda}L_B\right)} \quad (3)$$

where Z_{0B} is the characteristic impedance of the transmission line composed of the conductors A and B. The equivalent capacitance, C, can be estimated by

$$C = \frac{1}{j\omega Z_B}. \quad (4)$$

Figure 4 shows the antenna impedance at the natural resonant frequency of TM_{11} mode. The "conductor B model" means the result for the proposed structure shown in Fig. 1, and the "equivalent C model" means the results when the conductor B is removed and the equivalent capacitance is inserted between the conductor A and the probe. The reactance values for the both model have the almost same properties. Therefore, this part approximately acts as an open stub.

From the above investigations, the proposed antenna incorporating the open- and short- stubs, shown in Fig. 1, can be expressed approximately by the circuit model shown in Fig. 5. The series resonant circuit composed of the inductance due to the conductor A and the probe and the capacitance due to the conductor B, is loaded to the impedance of the MSA which has parallel-resonant characteristic. Hence, we can expect to increase the bandwidth of the MSA by incorporating the matching stubs.

4. EFFECT OF THE STUBS

In order to confirm and investigate the effect and influence of the stubs, the impedance characteristics and radiation pattern of the stubs-incorporated MSA are calculated. The dimensions are set to, H=0.048λ, L_A= 0.222λ, W_A=0.058λ, L_B=0.045λ, W_B=0.019λ, and H_A=H_B=0.010λ. The parameters of the stubs are chosen so as to widen bandwidth for VSWR<1.5. Figure 6 shows the comparison of the frequency characteristics of return-loss for the proposed antenna (with stubs) and the normal MSA (without stubs). The relative bandwidth (RBW) of 3.6% for VSWR<1.5 is obtained for the normal MSA. On the other hand, the RBW of 7.7% is achieved by incorporating the matching stubs into the normal MSA structure. It is about 2.1 times wider than the MSA without stubs in this case.

The radiation patterns at the center frequency are shown in Figs. 7 and 8. The beam-asymmetry in E-plane and the cross-polarization in H-plane would be mainly caused by the radiation from the feeding probe and from the shorting-post of the short-stub. The varying of the cross-polarization level can be seen. To clarify this phenomenon, the current distributions along the feeding probe and the shorting-post have been computed and are shown in Figs. 9 and 10. The relative phase difference between the two currents is approximately 180°. The integral values of each current along each conductor are not largely different from each other. We are considering that this is the reason why the cross-polarization level in H-plane degrades when adding the stubs.

5. CONCLUSION

We have proposed a novel MSA structure which has two stubs on the patch conductor to enhance the impedance-bandwidth. We have clarified that the two stubs mainly operate as the impedance-matching circuit. The effectiveness of the matching stubs on the bandwidth enhancement has been demonstrated numerically. Experimental verifications are our next important work.

REFERENCES

[1] R.V. Ketineni, U. Balaji and A. Das. "Improvement of bandwidth in microstrip antennas using parasitic patch", *Antennas and Propagat. Society International Symposium*, pp.1943-1947, Jul 1992.

[2] K. Araki, H. Ueda and T. Masayuki, "Numerical Analysis of Circular Disk Microstrip Antennas with Parasitic Elements", *IEEE Trans. Antennas and Propagat.*, vol. 34, No.12, pp.1390-1394, Dec 1986.

[3] R. Bhalla and L. Shafai, "Broadband patch antenna with a circular arc shaped slot", *Antennas and Propagat. Society International Symposium*, pp.394-397, Jun 2002.

[4] F. Yang, X-.X. Zhang, X. Ye and Y.R-. Samii, "Wide-Band E-Shaped Patch Antennas for Wireless Communications", *IEEE Trans. Antennas and Propagat.*, vol. 49, No.7, pp.1094-1100, Jul 2001.

[5] H.F. Pues and A.R.Van de Capelle, "An Impedance-Matching Technique for Increasing the Bandwidth of Microstrip Antennas", *IEEE Trans. Antennas and Propagat.*, vol. 37, No.11, pp.1345-1354, Jul 2001.
[6] K.M. Luk, C.L. Mak, Y.L. Chow and K.F. Lee, "Broadband microstrip patch antenna", *Electron. Lett.*, vol. 34, No.15, pp.1442-1443, Jul 1998.

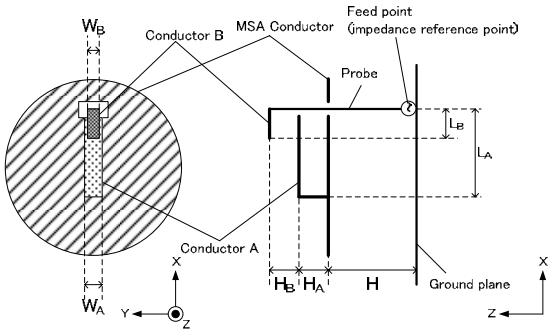

Fig. 1: Geometry of the antenna.

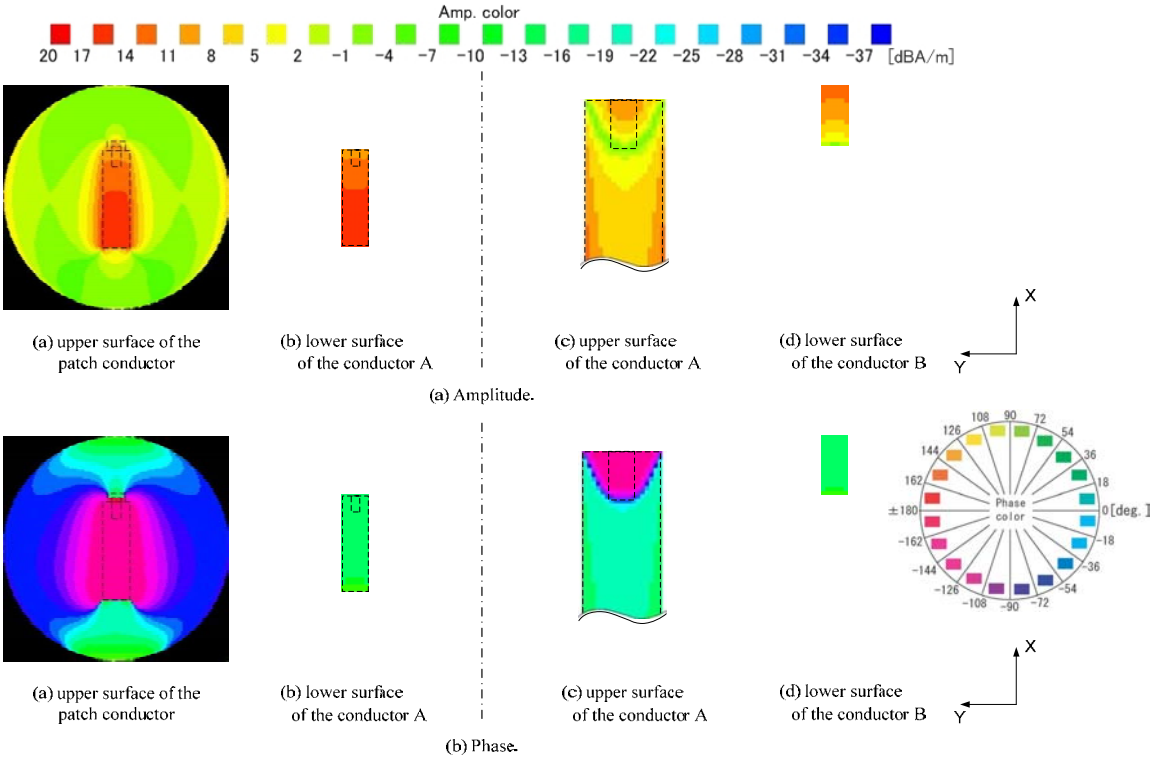

Fig. 2: Current distribution on the surface of each conductor.

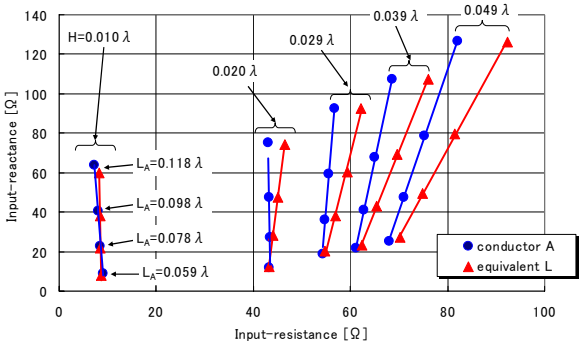

Fig. 3: Relationship between the antenna impedance at the natural resonant frequency of TM_{11} mode and L_A.

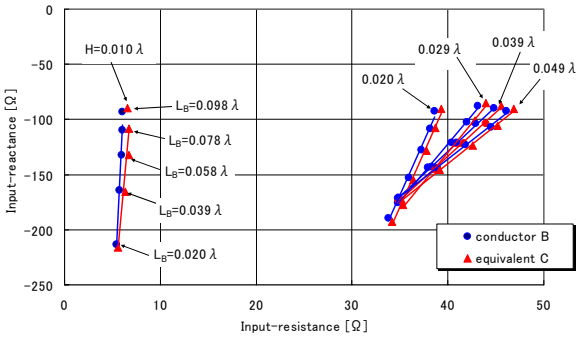

Fig. 4: Relationship between the antenna impedance at the natural resonant frequency of TM_{11} mode and L_B.

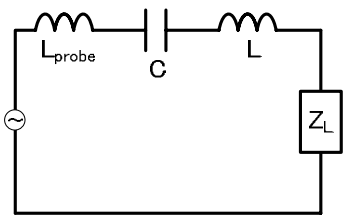

Fig. 5: The approximate circuit model. (Z_L and L_{probe} mean the antenna impedance without stubs and the probe's reactance, respectively.)

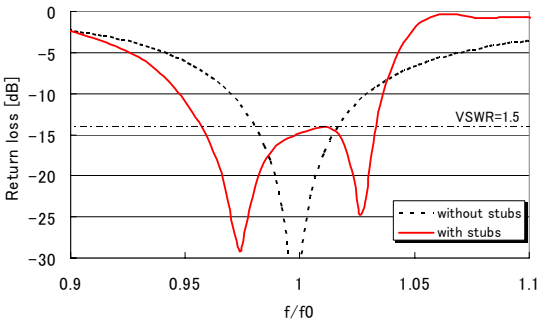

Fig. 6: Return loss vs. frequency for with or without stubs.

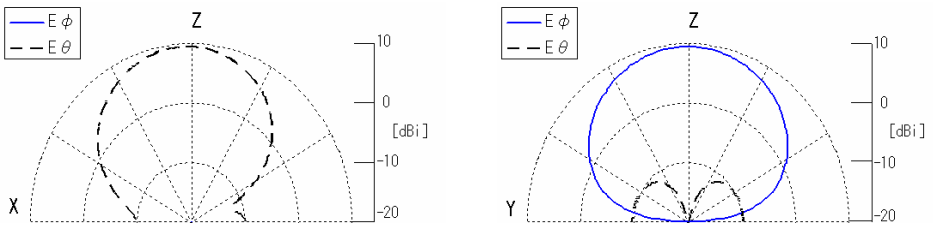

Fig. 7: Radiation pattern for the normal MSA (without stubs). The left figure is in E-plane and the right is in H-plane.

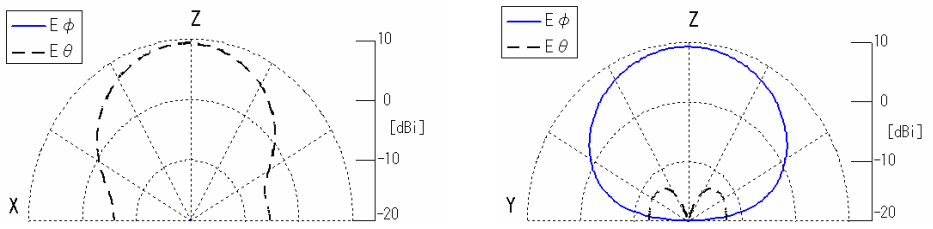

Fig.8: Radiation pattern for the stubs-incorporated MSA. The left figure is in E-plane and the right is in H-plane.

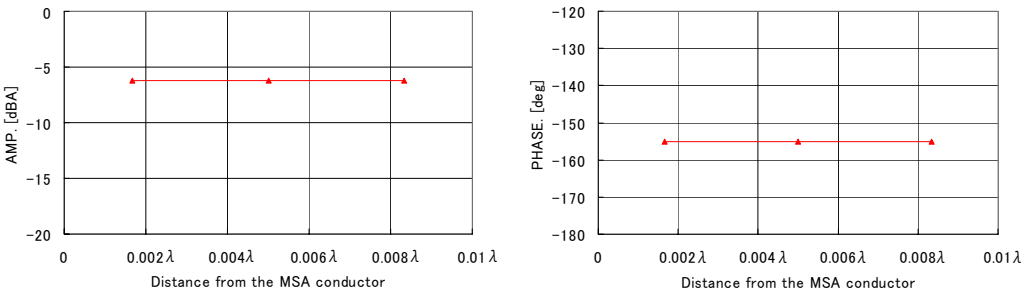

Fig. 9: Current distribution on the conductor connecting the patch conductor and the conductor A.

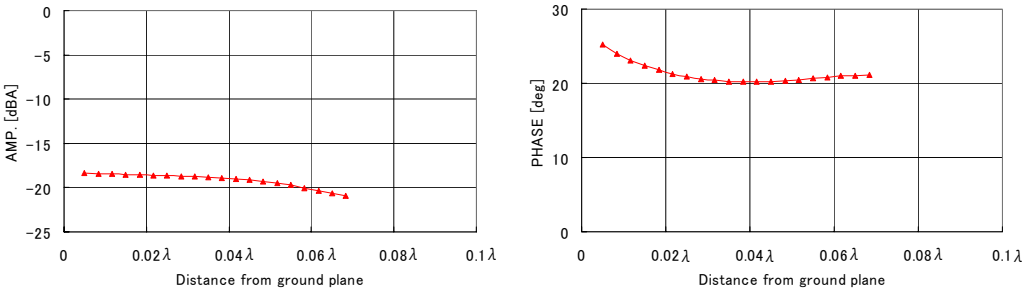

Fig. 10: Current distribution along the probe.